



# HHS Public Access

Author manuscript

*React Funct Polym.* Author manuscript; available in PMC 2017 March 01.

Published in final edited form as:

*React Funct Polym.* 2016 March 1; 100: 142–150. doi:10.1016/j.reactfunctpolym.2016.01.013.

## Surface modification of a polyethylene film for anticoagulant and anti-microbial catheter

Yingying Zheng<sup>a</sup>, Jianjun Miao<sup>b</sup>, Fuming Zhang<sup>b</sup>, Chao Cai<sup>b</sup>, Amanda Koh<sup>c</sup>, Trevor J. Simmons<sup>d</sup>, Shaker A. Mousa<sup>e</sup>, and Robert J. Linhardt<sup>b,\*</sup>

<sup>a</sup>Department of Physics and Key Laboratory of ATMMT Ministry of Education, Zhejiang Sci-Tech University, Hangzhou, 310018, People's Republic of China

<sup>b</sup>Department of Chemistry and Chemical Biology, Rensselaer Polytechnic Institute, Troy, New York, 12180-3590, USA

<sup>c</sup>Department of Chemical and Biological Engineering, Rensselaer Polytechnic Institute, Troy, New York, 12180-3590, USA

<sup>d</sup>Center for Future Energy Systems, Rensselaer Polytechnic Institute, Troy, New York, 12180-3590, USA

<sup>e</sup>The Pharmaceutical Research Institute, Albany College of Pharmacy, Albany, New York, 12208, USA

### Abstract

A functional anticoagulant and anti-bacterial coating for polyethylene (PE) films is described. The stepwise preparation of this nanocomposite surface coating involves O<sub>2</sub> plasma etching of PE film, carbodiimide coupling of cysteamine to the etched PE film, binding of Ag to sulfhydryl groups of cysteamine, and assembly of heparin capped AgNPs on the PE film. The nanocomposite film and its components were characterized by <sup>1</sup>H-nuclear magnetic resonance spectroscopy, attenuated total reflectance-Fourier transform infrared spectroscopy, X-ray photoelectron spectroscopy, and field emission-scanning electron microscopy. The resulting PE films demonstrate anticoagulant activity using a hemoglobin whole blood clotting assay, and anti-bacterial activity against *Bacillus cereus* 3551 (Gram-positive) and *Escherichia coli* BL21 (Gram-negative) bacteria. The hydrophilicity of the heparin coated PE was determined by contact angle measurements; and the stability of the nanocomposite film, with respect to Ag leaching, was assessed by atomic absorption spectroscopy.

### Keywords

polyethylene coating; anti-bacterial; anticoagulant; catheter; nanocomposite

---

\*Authors for correspondence R.J. Linhardt (Tel: 1-518-276-3404; linhar@rpi.edu).

**Publisher's Disclaimer:** This is a PDF file of an unedited manuscript that has been accepted for publication. As a service to our customers we are providing this early version of the manuscript. The manuscript will undergo copyediting, typesetting, and review of the resulting proof before it is published in its final citable form. Please note that during the production process errors may be discovered which could affect the content, and all legal disclaimers that apply to the journal pertain.

## 1. Introduction

The presence of an indwelling central venous catheter (CVC) is the strongest independent predictive factor for thrombosis in the arm [1] and is considered the main risk factor for occurrence of upper extremity deep vein thrombosis (UEDVT) [2]. The morbidity and mortality ranges from 15–50% and are statistically equivalent to lower extremity deep vein thrombosis [3, 4]. Post-thrombotic syndrome occurrence with DVT of the arm may be as high as one out of every three patients [5–7].

Radiographic studies show that up to 90% of cellular deposits form on the surface of the catheter, creating a fibrin sheath within the first 24 h after insertion [8]. Upper extremity thrombosis associated with peripherally inserted central catheters (PICCs) is becoming more common with the increased use of triple lumen catheters. Cancer patients with a CVC have greatly higher risk of developing UEDVT in the arm [9].

The relationship between thrombosis and infection has been established with significant colonization in areas of clot, and higher rates of catheter-related sepsis and catheter-related septicemia when thrombosis is present. In animal studies, fibrin sheath formation around central venous catheters significantly promoted colonization, catheter-related infection and persistent bacteremia [10–11].

According to the American College of Chest Physicians (ACCP Guidance, 2012), for most patients with UEDVT, catheter removal is not recommended if the device is functional and there is continued need for use. The damage associated with thrombosis is already done, but concerns over greater risk for infection remain. The rate of recurrence of upper extremity thrombosis if the catheter is removed and immediately placed into another site may be as high as 86% [12].

Catheters are used in many modern medical procedures [13], and a common use for catheters, such as a central venous catheter or Swan-Ganz catheter, involves their insertion into blood vessels [14]. The presence of such indwelling catheters can pose risks of blood clotting and infection [15–17]. Polymers used in making catheters are usually hydrophobic and often require lubrication to decrease damage on insertion into hydrophilic tissues [18]. In an effort to begin addressing these issues, our laboratory decided to investigate the use of stable hydrophilic nanocomposite coatings with anticoagulant and antibacterial properties.

Polyethylene (PE) based plastics are often used in the preparation of catheters [19]. Catheters are often made of the low-density PEs as these have more branching than high-density PEs and, thus, higher resilience. Because of these side branches, its molecules are less tightly packed and less crystalline. Low-density PE has a number of good performance characteristics, including transparency, flexibility, toughness, ease of processing, and an excellent ability for molding, making it suitable for use in catheters. PE, while having excellent mechanical properties, is quite hydrophobic [19], binds microbes [7, 8, 10, 11], and has poor blood compatibility, resulting in rapid clot formation [9]. While the direct non-covalent modification of PE with anticoagulant, anti-bacterial layers is possible, covalent modification should offer a more stable coating. Unfortunately, PE does not contain reactive functional groups onto which anticoagulant or antimicrobial agents can be covalently

attached. There are previous reports of introducing reactive functional groups onto the surface of PE films and catheters using O<sub>2</sub> plasma etching [20]. This modification introduces a surface layer of carboxyl groups onto PE that can allow for covalent attachment of a coating and increase the surface hydrophilicity without markedly changing the mechanical properties of the underlying PE.

The most commonly used anticoagulant is heparin, a polysaccharide-based drug that prevents blood from clotting by binding to the plasma protein antithrombin III (AT) and activating it against blood serine proteases, such as thrombin, that ultimately convert the soluble blood protein fibrinogen into an insoluble fibrin clot [21]. Heparin has been widely used to prepare coatings for catheters and other blood compatible devices used in medicine [21, 22].

There are many approaches for the preparation of anti-microbial and anti-bacterial coatings [23]. The most widely used approaches rely on molecules that non-specifically and rapidly kill microbes. Silver nanoparticles (NPs) have recently commanded much attention as effective broad-spectrum antimicrobial agents [24–29]. Since there are some concerns about the use of free silver nanoparticles because of their toxicity [30], attention has turned to immobilized Ag NPs [31].

A single nanocomposite [32], showing a combination of anticoagulant and anti-bacterial properties, has been previously explored by our laboratory [33, 34]. The current study examines the assembly of a covalently attached nanocomposite with hydrophilic coating on the surface of PE films, which exhibits both anticoagulant and anti-bacterial activities.

## 2. Experimental

### 2.1 Materials

Heparin sodium from porcine intestinal mucosa was purchased from Celsus Laboratories (Cincinnati, OH, USA). 2,6-Diaminopyridine (DAP), sodium cyanoborohydride, polyethylene (PE, average MW 35,000 determined by gel permeation chromatography (GPC) was selected for this study since it belongs to the class low-density PE and is suitable for the experiments undertaken in the current study), cysteamine (aminothioethanol), *N*-(3-dimethylaminopropyl)-*N*-ethylcarbodiimidehydrochloride (EDC), Drabkin's reagent and other common reagents were purchased from Sigma Chemicals (St. Louis, MO, USA) and used as received. Silver nitrate (AgNO<sub>3</sub>) was ordered from Amresco (Solon, OH, USA). *N*-hydroxysuccinimide (NHS) was from Thermo Scientific (Rockford, IL, USA). Dialysis membrane, 1000 molecular weight cutoff (MWCO), was from Spectrum Laboratories, Inc. (Houston, TX, USA). Glass slides were from Fisher Scientific (Pittsburg, PA, USA).

### 2.2 Surface modification of PE film (see Scheme 1)

**2.2.1 Synthesis of 2, 6-diaminopyridinyl heparin (DAPHP)**—The method of synthesizing 2, 6-diaminopyridinyl heparin (DAPHP) is described elsewhere in detail [35]. Briefly, heparin (500 mg, 41.5 μM) was dissolved in 15 mL formamide by heating at 50 °C. 2, 6-Diaminopyridine (500 mg, 4600 μM) was added and the reaction was maintained at 50

°C for 6 h. Aqueous sodium cyanoborohydride (47.5 mg, 750  $\mu\text{M}$ ) was added and the mixture was incubated at 50 °C for an additional 24 h. The reaction mixture was diluted with 50 mL of water and dialyzed against 2 L of water for 48 h using a 1000 MWCO dialysis membrane. The retentate was recovered, lyophilized, and purified by methanol precipitation three times. After the final precipitation, the precipitate was dissolved in water, dialyzed (1000 MWCO) against 2 L of water for 48 h twice, and lyophilized.

**2.2.2 Surface modification of PE film**—The PE film was prepared by cast melting. The polyethylene particles were put on a silicon wafer and heated at 160 °C. When melted, the PE was covered with a pre-cleaned microscope slide. The hot PE “sandwich” was immediately taken off the hot plate. After the PE cooled down sufficiently to solidify, the glass slide and silicon wafer were scraped with a razor blade to obtain a PE film having a thickness of  $\sim 0.5$  mm.

The PE films, thus prepared, were treated with oxygen plasma (oxygen pressure 0.5–1.2 torr) at a variety of power settings (30 watts, 50 watts, 100 watts) and for different lengths of time (30 s or 60 s) to afford surface carboxyl functionality using a TEGAL 411 plasma barrel stripper (Tegal Corp., Petaluma, California, USA). The oxygen plasma-activated, carboxyl-functionalized, PE film was then activated by immersing in an aqueous solution of 16 mmol/mL EDC and 16 mmol/mL NHS, and gently shaken for 1 h. When the reaction was completed, the films were then transferred into aqueous solution of cysteamine (0.05 M) and shaken for another 3 h. PE films modified with thiol functional groups on their surface were obtained and subsequently transferred into  $\text{AgNO}_3$  solution (140 mM) for 1 h incubation to bind  $\text{Ag}^+$  ions to the thiol groups.

PE-Ag nanoparticles (NPs) were synthesized by reduction with DAPHP [33]. The PE films were placed standing upright in a flask. DAPHP aqueous solution (reducing agent) was then added into the system (0.5 mM solution) and the mixture was heated at 95 °C for 4 h. The PE films changed color to brown indicating the growth of AgNPs. Afterwards, clear DAPHP-AgNPs coated PE films were obtained after three-time wash with water and air-dried.

### 2.3 Characterization

The  $^1\text{H}$  NMR spectra were obtained on a Bruker 600 MHz spectrometer (Bruker, Switzerland) with Topspin 2.1 software. All measurements were performed at 298 K, using the pulse accumulation of 64 scans and LB parameter of 0.30 Hz. Deuterium oxide ( $\text{D}_2\text{O}$ ) was used as the solvent for DAPHP. Attenuated total reflectance Fourier transform infrared (ATR-FTIR) spectra were collected with a PerkinElmer Spectrum One Spectrometer (PerkinElmer, Inc. Waltham, Massachusetts, USA) using the Diffuse Reflectance sampling accessory with a Zinc Selenide internal reflection element (IRE). These spectra were collected using rapid-scan software spectrum v5.3.0 with 8 scans and a resolution of  $4\text{ cm}^{-1}$ . X-ray photoelectron spectroscopy (XPS) measurements were carried out in a PHI 5400 instrument with a 102 W Al KR probe beam. The spectrometer was configured to operate at high resolution with a pass energy of 20 eV. Samples were imaged using a field emission scanning electron microscope (FE-SEM) of a Zeiss SUPRA-55 instrument (Oberkochen,

Germany). All samples were sputter-coated with 1 nm of Pt (Denton Vacuum Desk IV, Moorestown, NJ) prior to imaging. Images were obtained at a working distance of 2.8–4.7 mm using an acceleration voltage of 2 kV or 10kV. Energy dispersive X-ray (EDX) microanalysis was performed on Oxford INCA EDS System 250 equipped in a FE-SEM Zeiss SUPRA-55. The electron beam was operated at 15 kV.

**2.3.1 Anticoagulant activity of the film surface**—Anticoagulant activity was determined by using a hemoglobin (Hb) assay to measure the hemoglobin content in the red fibrin clot formed on the PE film after applying smear of human whole blood. The negative (–) control film (unmodified PE) showed the highest Hb concentration and the positive (+) control film (PE with heparin) showed Hb concentrations approaching zero. Using 96-well plate plastic sealers, PE films (unmodified, treated with O<sub>2</sub> plasma or coated with DAPHP-AgNPs) were cut into dimensions of 2 cm × 2 cm and were placed into 6-well, sterile, clear, tissue culture plates. For (+) control samples, 50 μL of known concentrations of heparin (0.6 mg/mL, 0.9 mg/mL, 1.5 mg/mL) were added onto each unmodified PE film. Whole human blood (25 μL), collected in 10 ml untreated (no anticoagulant) sterile collection tubes using aseptic technique, was placed on each film. The 25 μL blood droplet was spread evenly across film with sterilize inoculating needle. The samples were incubated on bench top for 15 min (the time required to form blood clot on the (–) control film). The films were washed with sterile water to remove unattached/un-clotted blood. The films with blood clots were placed in 2 mL sterile tubes and stored overnight at 4 °C. Clots were homogenized the next day using Fisher Scientific Power Gen 1000 cell homogenizer (per protocol). Hemoglobin levels were measured using Sigma Aldrich Drabkin's reagent (per protocol) [36]. Supernatant, 50 μL from homogenized sample, was diluted in 200 μL of Drabkin's reagent to prepare a working sample for analysis. The absorbance of the prepared samples was tested for the quantitative colorimetric determination of blood hemoglobin.

**2.3.2 Quantification of DAPHP immobilized on PE film**—The quantification of DAPHP immobilized on PE film was determined by disaccharide analysis using the liquid chromatography-mass spectrometry (LC-MS) as previously reported [37]. Briefly, DAPHP-AgNPs coated PE films (two pieces of 0.4 × 0.4 cm<sup>2</sup>) were prepared and DAPHP on the surface of the PE films was completely depolymerized using a mixture of heparin lyases (I, II, and III) and then the heparin-derived disaccharides were collected by YM-10 spin column and freeze-dried. The PE film treated with oxygen plasma was used as the negative control. The freeze-dried heparin-derived disaccharides or a mixture of 8 HS/HP disaccharide standards were labeled with 2-aminoacridine (AMAC). The AMAC-tagged disaccharide standards were diluted to different concentrations (0.5–100 ng per sample) using aqueous DMSO and LC-MS analyses (Agilent 1200 LC/MSD (Agilent Technologies, Inc. Wilmington, DE) equipped with a 6300 ion-trap and a binary pump) was performed. Quantification analysis of disaccharides was performed using calibration curves established by separation of increasing amounts of unsaturated disaccharide standards (0.1, 0.5, 1, 5, 10, 20, 50, 100 ng/each). Linearity was assessed based on the amount of disaccharide and peak intensity in extracted ion chromatogram (EIC).

**2.3.3 Anti-bacterial activity of the film surface**—The anti-bacterial activity of the film surface was evaluated by means of a slightly modified protocol based on the Japanese Industrial Standard method (JISZ 2801:2000). Bacteria were grown by taking 10  $\mu\text{L}$  of frozen bacteria strains (*Bacillus cereus* 3551 (Gram-positive) or *Escherichia coli* BL21 (Gram-negative)) into 3 mL of Nutrient Broth (NB) medium for *Bacillus cereus* or Lysogeny Broth (LB) medium for *Escherichia coli*, and incubating overnight at 37 °C on a shaker. 20  $\mu\text{L}$  of overnight culture were transferred to 3 mL of fresh NB or LB medium, allowing these to grow for 4 h. The growth was monitored by a spectrophotometer at OD600 by diluting 1:5 into NB or LB medium. The blank was NB or LB medium. When OD600 reached 0.6–0.8, it indicates that the bacteria are in the mid-log phase. The mid-log phase culture of *Bacillus cereus* or *Escherichia coli* were centrifuged at 12,000 rpm (13,400  $\times$  g) for 2 min using Eppendorf Centrifuge 5415D and re-suspended in phosphate buffered saline (PBS) at the final concentration of  $5.0 \times 10^8$  CFU  $\text{mL}^{-1}$  for *Bacillus cereus* 3551 and  $8.0 \times 10^8$  CFU  $\text{mL}^{-1}$  for *Escherichia coli* BL21. 10  $\mu\text{L}$  of each bacterial suspension were deposited on each DAPHP-AgNPs coated or uncoated square PE film ( $20 \times 20$   $\text{mm}^2$ ), and covered with UV sterilized uncoated square PE sheets ( $10 \times 10$   $\text{mm}^2$ ). The “sandwich” was incubated for 40 min at 37 °C under saturated humidity. At the end of incubation, the samples were immersed in 5 mL of PBS and vigorously vortexed for 30 s to allow the detachment of bacteria from the support. After proper serial dilutions in PBS, the bacterial suspensions were plated on NB agar for *B. cereus* 3551 or LB agar for *E. coli* BL21 and incubated overnight at 37 °C to allow the viable colony counts. The values reported are the mean  $\pm$  standard deviation of three independent experiments with comparable results.

**2.3.4 Hydrophilic experiment**—Static air–water contact angle (WCA) was measured using drop shape analyzer Germany Kruss DSA-100 (comp. method: Laplace-Young) at ambient humidity and temperature. A 10  $\mu\text{L}$  of distilled water droplet was placed on the PE film sample surface, using a micro-syringe, and it was imaged using a CCD camera. The contact angle was then measured directly from the computer-generated image of the water droplet and calculated via the software provided with the instrument. The values reported are the average of three independent experiments with comparable results.

**2.3.5 Release characteristics of AgNPs**—The concentration of AgNPs released in a releasing medium (distilled water, or simulated body fluid (SBF)) from the DAPHP-AgNPs coated PE films was measured by atomic absorption spectroscopy (AAS) using a Perkin-Elmer Model 3100 AAS. The results were reported as average values ( $n = 3$ ). Prior to the release assay, the actual amount of AgNPs on the DAPHP-AgNPs coated PE film (rectangle:  $2.0 \times 1.0$   $\text{cm}^2$ ) was determined. The actual amount of Ag was quantified by treating each film specimen with 2 mL of 95% nitric acid ( $\text{HNO}_3$ ), followed by the addition of a releasing medium (distilled water or SBF) to attain a total volume of 12 mL.

The DAPHP-AgNPs coated PE films (rectangle:  $3.5 \times 2.5$  cm) were immersed in 12 mL of the releasing medium (distilled water or SBF) and were shaken in a shaking incubator at 220 rotations/min at physiological temperature, 37 °C, to simulate the local *in vivo* release conditions. Aliquots were withdrawn from these solutions at fixed time intervals of 1 h, 5 h, 10 h, 1 d, 2 d, 5 d, and 10 d for determination of Ag release and the equivalent volumes of

fresh deionized water or SBF were added into the containers after each sampling to maintain constant medium volume. At each time point, the measurements were carried out in triplicate. The cumulative amount of released AgNPs was calculated from the data obtained using AAS spectrometry.  $\text{HNO}_3$  was added to the aliquots prior to AAS analysis to ensure that all Ag existed as the ionic species. The measurements were calibrated with a standard curve from 0–4 mg/L using an  $\text{AgNO}_3$  standard solution. The control DAPHP-AgNPs coated PE film treated with 95%  $\text{HNO}_3$  yielded 0.175 mg/L. All other samples evaluated showed values equivalent to zero independent of shaking time or solution composition.

### 3. Results and discussion

#### 3.1 Surface modification on PE film

Heparin (HP) has reactive aldehyde groups at its reducing end which offers a convenient handle by which heparin can be derivatized for covalent attachment to a variety of matrices. In this paper, 2, 6-diaminopyridinyl heparin (DAPHP) was obtained through the coupling of heparin to 2, 6-diaminopyridine (DAP) by reductive amination [35].  $^1\text{H}$  NMR confirmed the reductive amination of heparin, as the resulting DAPHP showed three aromatic proton signals at 6.09 ppm ( $\text{H}^a$ ), 7.45 ppm ( $\text{H}^b$ ) and 8.0 ppm ( $\text{H}^c$ ) corresponding to 2,6-diaminopyridine as expected (Fig. 1).

Scheme 1 shows the stepwise modification of the PE film. The PE film was first treated with  $\text{O}_2$  plasma to functionalize carboxylic acid groups. The carboxyl groups on the PE film were activated with EDC/NHS to form a carbodiimide intermediate, which was used for the assembly to cysteamine by carboxyl-amine coupling. Afterwards, the silver ions ( $\text{Ag}^+$ ) were chemisorbed onto the PE film surface modified by thiol functional groups. Ag nanoparticles (NPs) were prepared using heparin derivative (DAPHP) [33]. It is believed that the aldehyde functional groups at the reducing ends of the residual un-derivatized heparin present in DAPHP reduce  $\text{AgNO}_3$  to AgNPs and the amino/pyridine group of the DAPHP provides a strong interaction with the resulting AgNPs. DAPHP-AgNPs coated PE films with both anticoagulant heparin and antimicrobial AgNPs were successfully achieved. The optical image of the PE film after coating with AgNPs showed a characteristic brown color consistent with the presence of AgNPs (Fig. 2). The color of Fig. 2 (b) is relatively uniform although the edges are darker and there are some aggregated dark brown spots. The darker edge likely results from its unique location when the PE film undergoes a series of treatment in the small-scale reaction. The aggregated dark brown spots may be due to our handling of the PE film with tweezers. The stability of the AgNPs bound to the film results from their covalent interaction with the thiol ( $-\text{SH}$ ) on PE film. Sulfhydryl and amino groups are known to bind to Ag strongly and can control the size and morphology of the particles [38].

The structural properties of the PE film (Fig. 3(a)), the PE film treated with  $\text{O}_2$  plasma (Fig. 3(b)) and the DAPHP-AgNPs coated PE film (Fig. 3(c)) were investigated by ATR-FTIR. The characteristic absorption peaks at about  $2916\text{ cm}^{-1}$ ,  $2850\text{ cm}^{-1}$ ,  $1463\text{ cm}^{-1}$  and  $720\text{ cm}^{-1}$  result from polyethylene C-H and C-C absorption in the IR region. After  $\text{O}_2$  plasma treatment, the PE film showed two new peaks at  $3429\text{ cm}^{-1}$  and  $1582\text{ cm}^{-1}$ , which belong to H-O and carboxyl stretching vibrations (Fig. 3(b)). The characteristic absorption peaks at  $1150\text{ cm}^{-1}$  and  $1239\text{ cm}^{-1}$  are assigned to the symmetric and asymmetric stretching

vibrating of heparin's O=S=O group [39] (Fig. 3(c)). The peak at  $1239\text{ cm}^{-1}$  is attributed to the C–O stretch in –COOH in the heparin molecule. Also, the band at  $1030\text{ cm}^{-1}$  was assigned to the –SO<sub>3</sub> group [40] of heparin, allowing the presence of heparin molecules on the DAPHP-AgNPs coated PE film to be established.

The PE film treated with O<sub>2</sub> plasma and the DAPHP-AgNPs coated PE film were next analyzed by XPS. The general scan spectrum showed the presence of the principal C1s, N1s, O1s, S2p, and Ag3d core levels for DAPHP-AgNPs coated PE film with no evidence of impurities. C1s, N1s, O1s, S2p, and Ag3d core levels from these films are shown in Fig. 4. For PE film and PE film treated with O<sub>2</sub> plasma, there is only one C1s core level peak at 284 eV (Fig. 4(a)), while for DAPHP-AgNPs coated PE film, three C1s core level peaks at 284 eV, 285 eV, and 287 eV appeared because of the introducing of the DAPHP. The higher two core level peaks (285 eV and 287 eV) are assigned to the electron emission from the advantageous carbon and the carbons coordinated to hydroxyl and carboxylic groups, respectively, in heparin molecules. For the PE film, a small O1s core level peak (531 eV) appeared, which is consistent with literature reports of a detectable oxygen impurity (Fig. 4(b)). After the surface of PE film was treated with O<sub>2</sub> plasma, the O1s peak (531 eV) became bigger indicating the formation of carboxyl groups. For DAPHP-AgNPs coated PE film, a new peak (532 eV) appeared due to the introduction of DAPHP. N 1s band is not observed for PE film and PE film treated with O<sub>2</sub> plasma (Fig. 4(c)). For DAPHP-AgNPs coated PE film, N 1s band at 399 eV appeared corresponding to the nitrogen atom of DAPHP molecules attached to AgNPs. There are two peaks (161 eV, 168 eV) of S2p core level for DAPHP-AgNPs coated PE film (Fig. 4(d)). 161 eV comes from C-S-Ag, while 168 eV comes from R-SO<sub>3</sub>- of DAPHP, revealing the existence of S-Ag and DAPHP molecules. The binding energies of Ag in DAPHP-AgNPs film (Fig. 4(e)) were 367.4 eV (3d<sub>3/2</sub>) and 373.4 eV (3d<sub>5/2</sub>), which were lower than those of elemental silver (368.4 eV and 374.4 eV), because of the interaction between the thiol and amino and silver.

### 3.2 Film morphology

SEM analysis reveals the size and shape of the AgNPs bound to the PE films. Based on these images the AgNPs equably coated onto the surface of PE film showed a uniform and mono-disperse size and shape. Sparse and small AgNPs (10–20 nm) were coated on the PE film when the O<sub>2</sub> plasma treatment was incubated for 1 min at 30 W (Fig. 5(a)). When the O<sub>2</sub> plasma treatment was enhanced to 50 W, a larger (40–50 nm) and denser AgNP coating was obtained (Fig. 5(b)). This behavior may be attributed to the different degrees of attraction of SH groups toward Ag<sup>+</sup> ions. The attraction between SH groups and Ag<sup>+</sup> ions can be considered as a stronger chemical bond, which can control their size and morphology of the particles. Based on SEM results, we suspect that the SH groups on the PE film acted as nucleation and growth sites for the AgNPs. When higher power of O<sub>2</sub> plasma was used in the modification process, more carboxyl groups were introduced and more sulfuryl groups were presented on the surface of PE film, which provided more nucleation and growth sites. The smoothness of the nanoparticles indicates that a DAPHP film seems to wrap the particles around. High magnification images (Fig. 5(b), inset) show that the AgNPs are covered with a thin film that corresponds to DAPHP. Energy-dispersive X-ray analysis (EDX) (Fig. 5(c)) confirmed the presence of silver and successful attachment of heparin to



the AgNPs surfaces in terms of the appearance of the peaks for S, O, and Na. DAPHP contains a diaminopyridine moiety that can bind tightly to the surface of newly formed AgNPs.

### 3.3 Anticoagulant activity of film surface

The anticoagulant activity of DAPHP-AgNPs coated PE film is most commonly determined by using a hemoglobin (Hb) assay to measure hemoglobin content in the red fibrin clot formed on the PE film after applying smear of human whole blood. A standard curve demonstrates that as the hemoglobin (Hb) solution concentration increases the absorbance decreases, corresponding to a decreased fibrin clot (Table 1). Excellent linearity was observed using this assay (Fig. 6(a)).

The anticoagulant activity of DAPHP-AgNPs coated PE film was compared with unmodified PE film (negative control) and free heparin molecules (positive control) (Table 2 and Fig. 6(b)). The unmodified PE film (blank) has the highest Hb. The Hb decreased with the increase amount of the free heparin. When 1.5-mg/mL heparin was added, Hb concentration is no detectable (OD blank = 0.002) which means the red fibrin clot do not formed on the PE film because of the free heparin. The in vitro data of PE film treated with O<sub>2</sub> plasma also clearly indicate the contribution of plasma treatment, which makes the PE film have a more hydrophilic surface in the inhibition of coagulation. The result of this study showed that the film containing immobilized DAPHP had approximately the same anticoagulant activity as 50  $\mu$ L of 1.4 mg/mL of free heparin added onto the unmodified PE film. Almost no Hb can be tested (OD blank = 0.008).

The amount of heparin loaded on the DAPHP-AgNPs coated PE film is quantified using the disaccharide analysis by LC-MS after heparin lyases digestion. As shown in Fig. 7, for the PE film treated with O<sub>2</sub> treatment (as the negative control), no disaccharide peak was shown in the extracted ion chromatograph (EIC) (Fig. 7(c)). The EIC of DAPHP-AgNPs coated PE film (Fig. 7(d)) is consistent with the EIC of standard heparin (Fig. 7(b)), and the quantified amount of DAPHP loading on PE film is 2.4225  $\mu$ g heparin/cm<sup>2</sup> PE film (0.775  $\mu$ g total for 2 $\times$ 0.4 $\times$ 0.4 cm<sup>2</sup>), which is much less than 17.5  $\mu$ g heparin / cm<sup>2</sup> PE film for 50  $\mu$ L of 1.4 mg/mL of heparin added on the unmodified PE film (2 $\times$ 2cm<sup>2</sup>) but has the same anticoagulant properties.

Other parameters as well were determined. The blank PE film without heparin coating formed a firm red clot within 15 min but for 1.5 mg/mL heparin coated PE film and DAPHP-AgNPs coated PE film, it took more than 6 h for clot to form firmly. Previously, we demonstrated the synthesis of AgNPs, using heparin and DAPHP as both reducing and stabilizing agent, which showed effective anticoagulant and anti-inflammatory efficacy [33]. End point attachment of a heparin derivative to an aminated support show better antithrombin binding efficiency than non-directionally immobilized heparin [35].

### 3.4 Anti-bacterial evaluation of film surface

Nanomaterials have been exploited from their anti-bacterial applications in biomedical [24–29, 32] and in food packaging applications [41]. Anti-bacterial assessment was carried out

with two different bacterial species, *B. cereus* 3551 (Gram +) and *E. coli* BL21. (Gram –). Each bacterium was uniformly applied to the surface of the DAPHP-AgNPs coated PE film and uncoated PE film (control). After 40 min of incubation, bacteria were detached from the samples and the number of colony forming units (CFU mL<sup>-1</sup>) was evaluated. *In vitro* results showed that the nanocomposite coating is effective in killing both bacterial strains, with a drop of almost six orders of magnitude in the CFU mL<sup>-1</sup>, while the uncoated PE control displayed no anti-bacterial effect (Fig. 8). This is consistent with the known antibacterial activity of immobilized AgNPs. This result could be explained by the small particle size, which leads to greater surface area and more effective antimicrobial activity.

### 3.5 Surface Hydrophilicity

The water contact angle (WCA) above 90° can be called a hydrophobic surface, while surfaces with a WCA less than 90° are hydrophilic. WCA measurement shows a decrease of PE film on O<sub>2</sub> plasma etching and a further and more substantial decrease on the modification of the surface with DADHP (Fig. 9). The contact angle data indicate that O<sub>2</sub> plasma treatment and the immobilized DAPHP both contribute to the increase in wettability of PE film surface. Adherent hydrophilic coatings provide catheters with a “slippery-when-wet” lubricious surface. Hydrophilic surfaces can reduce the adsorption of fibrin and the aggregation of the blood platelet, which improve the anticoagulation properties. Moreover, hydrophilic surfaces can also reduce bacterial adherence, which increases the anti-bacterial activity as well.

Hydrophilic surfaces can reduce patient trauma and decrease friction caused on inserting a catheter into the body to avoid severe mechanical trauma. Hence, this newly designed PE film could be applied to the medical catheter associated with a reduction of tissue injury.

### 3.6 Release characteristic of as-loaded silver

AgNPs with a high ratio of surface area per unit mass are of interest because they offer slow, controlled release. The results suggest that some DAPHP polysaccharide molecules bind the bio-conjugate via weak electrostatic interaction and that these free polysaccharides can be desorbed from the surface of bio-conjugate on repeated washing.

## 4. Conclusions

Even a small percentage occurrence of thrombosis or infection is significant to patient morbidity and increased cost, given that there are more than six million CVCs inserted each year in the United States alone, and that two million of those are PICCs. There appears to be a close association between catheter-related thrombosis and catheter-related infection. In the Oncology patient, the risk of infection and thrombosis is even more pronounced. Hence, it is important to utilize strategies to prevent catheter-related thrombosis and catheter-related infection. The anticoagulant properties of the silver-heparin PE films come primarily from the effect of heparin, although the Ag loading and WCA may make some secondary contributions. The AgNPs and to a lesser degree the increased hydrophilicity as demonstrated from the WCA clearly provide the anti-infective activity of these films. Our results demonstrate the potential in developing a film for catheter manufacturing that would

overcome catheter-associated infection and thrombosis, which will be carried out in further studies.

## Supplementary Material

Refer to Web version on PubMed Central for supplementary material.

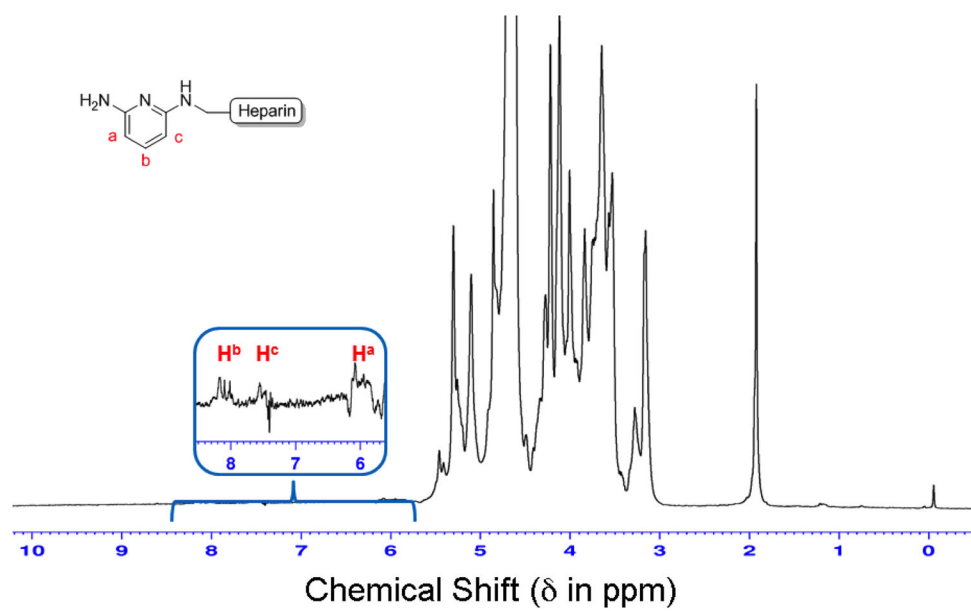
## Acknowledgments

This work was partially supported by a grant from the China Scholarship Council and Zhejiang Sci-Tech University along with the Zhejiang Provincial Natural Science Foundation of China (No. LY15E030011). This research was funded by a grants from the National Institutes of Health # HL62244 and HL096972.

## References

1. Joffe HV, Kucher N, Tapson VF, Goldhaber SZ. *Circulation*. 2004; 110:1605–1611. [PubMed: 15353493]
2. Flinterman LE, Van Der Meer FJ, Rosendaal FR, Doggen CJ. *J Thromb Haemost*. 2008; 6:1262–1266. [PubMed: 18485082]
3. Mai C, Hunt D. *Am J Med*. 2011; 124:402–407. [PubMed: 21531227]
4. Spencer FA, Emery C, Lessard D, Goldberg RJ. *Am J Med*. 2007; 120:678–684. [PubMed: 17679126]
5. Evans RS, Sharp JH, Linford LH, et al. *Chest*. 2010; 138:803–810. [PubMed: 20923799]
6. Verso M, Agnelli G. *J Clin Oncol*. 2003; 21:3665–3675. [PubMed: 14512399]
7. Timsit JF, Misset B, Carlet J, et al. *Chest*. 1998; 114:207–213. [PubMed: 9674471]
8. Wechsler RJ, Spirn PW, Conant EF, Steiner RM, Needleman L. *Am J Roentgenol*. 1993; 160:467–471. [PubMed: 8430537]
9. Blom JW, Doggen CJM, Osanto S, Rosendaal FR. *J Thromb Haemost*. 2005; 3:2471–2478. [PubMed: 16241945]
10. Mehall JR, Saltzman DA, Jackson RJ, Smith SD. *Crit Care Med*. 2002; 30:908–912. [PubMed: 11940768]
11. Raad II, Luna M, Khalil SM, Costerton JW, Lam C, Bodey GP. *JAMA*. 1994; 271:1014–1016. [PubMed: 8139059]
12. Jones MA, Lee DY, Segall JS, et al. *J Vasc Surg*. 2010; 51:108–113. [PubMed: 19879094]
13. Wilson KM. *Nursing*. 2013; 43:66–68. [PubMed: 24257535]
14. Berry D, William VG. 1919–2009, cardiologist and co-inventor of the Swan-Ganz catheter which revolutionized cardiovascular investigations. *Eur Heart J*. 2011; 32:660–661. [PubMed: 21523942]
15. Geffers C, Gastmeier A, Schwab F, Groneberg K, Rüden H, Gastmeier P. *Infect Cont Hosp Ep*. 2010; 31:395–401.
16. Khorana AA. *Ann Oncol*. 2009; 20:619–1630.
17. Mermel LA, Allon M, Bouza E, Craven DE, Flynn P, O'Grady NP, Raad II, Rijnders BJA, Sherertz RJ, Warren DK. *Clin Infect Dis*. 2009; 49:1–45. [PubMed: 19489710]
18. Birmingham SL, Hodgkinson S, Wright S, Hayter E, Spinks J, Pellowe C. *BMJ*. 2013; 8:346.
19. Swahn B, Gunne I. *Ann Radiol (Paris)*. 1979; 22:356–357. [PubMed: 496283]
20. Guruvenket S, Rao GM, Komath M, Raichur AM. *Appl Surf Sci*. 2004; 236:278–284.
21. Linhardt RJ. *J Med Chem*. 2003; 46:2551–2554. [PubMed: 12801218]
22. Murugesan S, Xie J, Linhardt RJ. *Curr Top Med Chem*. 2008; 8:80–100. [PubMed: 18289079]
23. Salwiczek M, Qu Y, Gardiner J, Strugnell RA, Lithgow T, McLean KM, Thissen H. *Trends Biotechnol*. 2014; 32:82–90. [PubMed: 24176168]
24. Chaloupka K, Malam Y, Seifalian AM. *Trends Biotechnol*. 2010; 28:580–588. [PubMed: 20724010]
25. Knetsch MLW, Koole LH. *Polymers*. 2011; 3:340–366.

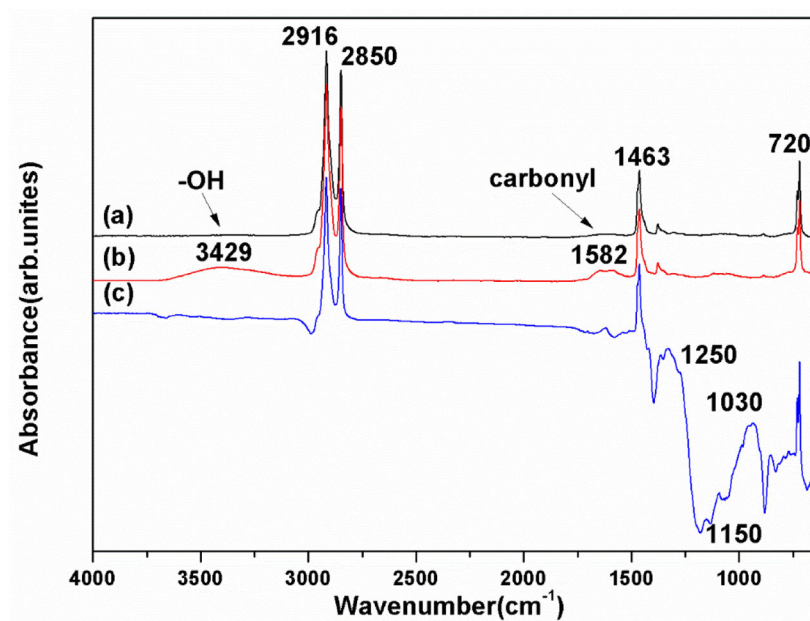
26. Rai M, Yadav A, Gade A. *Biotechnol Adv.* 2009; 27:76–83. [PubMed: 18854209]
27. Shrivastava S, Bera T, Roy A, Singh G, Ramachandrarao P, Dash D. *Nanotechnology.* 2007; 18:225103–225112.
28. Samuel U, Guggenbichler JP. *Int J Antimicrob Agents.* 2004; 23:75–78.
29. Hsu SH, Tseng HJ, Lin YC. *Biomaterials.* 2010; 31:6796–6808. [PubMed: 20542329]
30. You C, Han C, Wang X, Zheng Y, Li Q, Hu X, Sun H. *Mol Biol Rep.* 2012; 39:9193–9201. [PubMed: 22722996]
31. Lin JJ, Lin WC, Li SD, Lin CY, Hsu SH. *ACS Appl Mater Interfaces.* 2013; 5:433–443. [PubMed: 23270500]
32. Zheng Y, Monty J, Linhardt RJ. *Carbohydr Res.* 2015; 405:23–32. [PubMed: 25498200]
33. Kemp MM, Kumar A, Mousa S, Park TJ, Ajayan P, Kubotera N, Mousa SA, Linhardt RJ. *Biomacromolecules.* 2009; 10:589–595. [PubMed: 19226107]
34. Kemp M, Kumar A, Clement D, Ajayan P, Mousa S, Linhardt RJ. *Nanomed.* 2009; 4:421–429.
35. Nadkarni VD, Pervi A, Linhardt RJ. *Anal Biochem.* 1994; 222:59–67. [PubMed: 7856872]
36. Makarem, A. Hemoglobins, Myoglobins, and Haptoglobins. In: Henry, RJ., et al., editors. *Clinical Chemistry - Principles and Technics.* 2. Harper & Row; Hagerstown, MD: 1974. p. 1128-1135.
37. Yang B, Chang Y, Weyers AM, Sterner E, Linhardt RJ. *J Chromatogr.* 2012; 1225:91–98.
38. Sinclair T, Zieba M, Irusta S, Sebastián V, Arruebo M. *Nanotechnology.* 2014; 25:305101–305113. [PubMed: 25006109]
39. Martins AF, Pereira AGB, Fajardo AR, Rubira AF, Muniz EC. *Carbohydr Polym.* 2011; 86:1266–1272.
40. Wang J, Hu W, Liu Q, Zhang S. *Colloid Surface B.* 2011; 85:241–247.
41. Sundramoorthy AK, Gunasekaran S. *Trends Anal Chem.* 2014; 60:36–53.



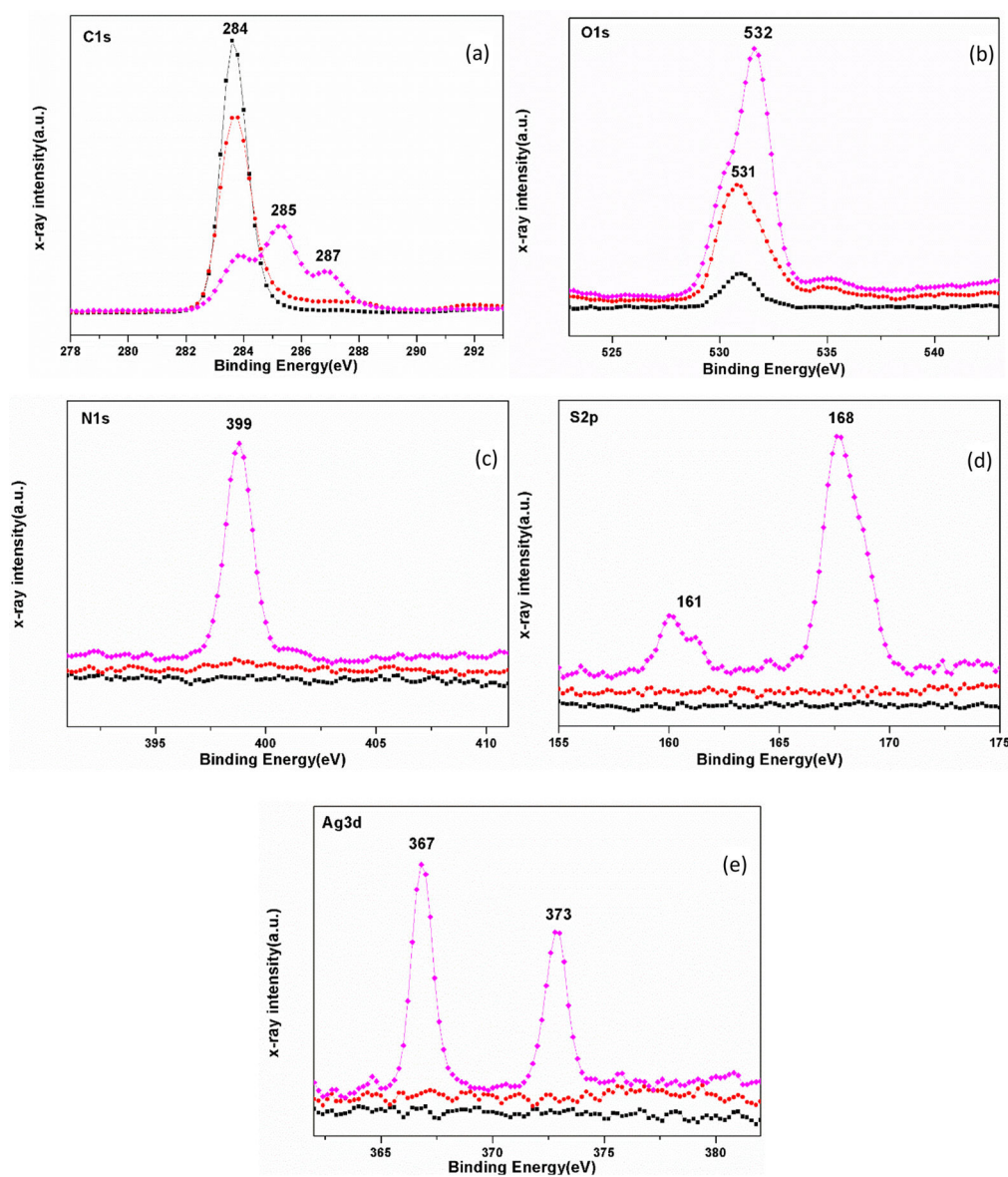
**Fig. 1.**  
 $^1\text{H}$  NMR of DAPHP.



**Fig. 2.**  
Optical image of PE film (a) and DAPHP-AgNPs coated PE film (b).

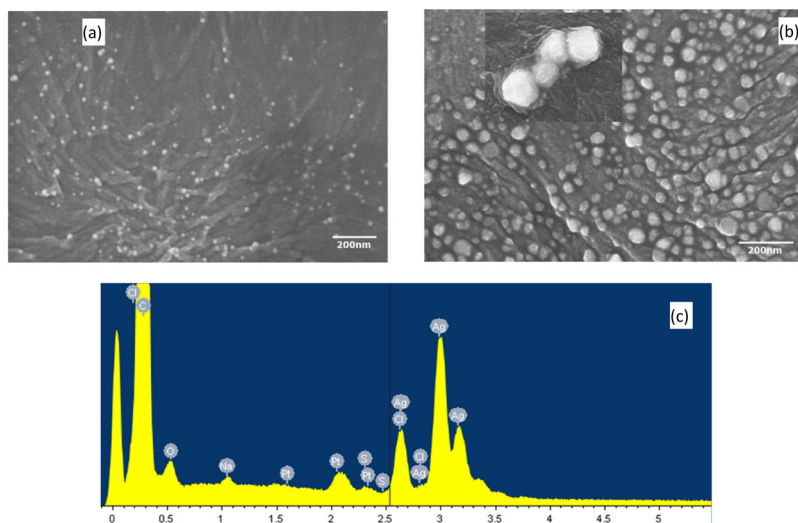


**Fig. 3.** ATR- FTIR spectra of (a) PE film; (b) PE film treated with O<sub>2</sub> plasma; (c) DAPHP-AgNPs coated PE film.

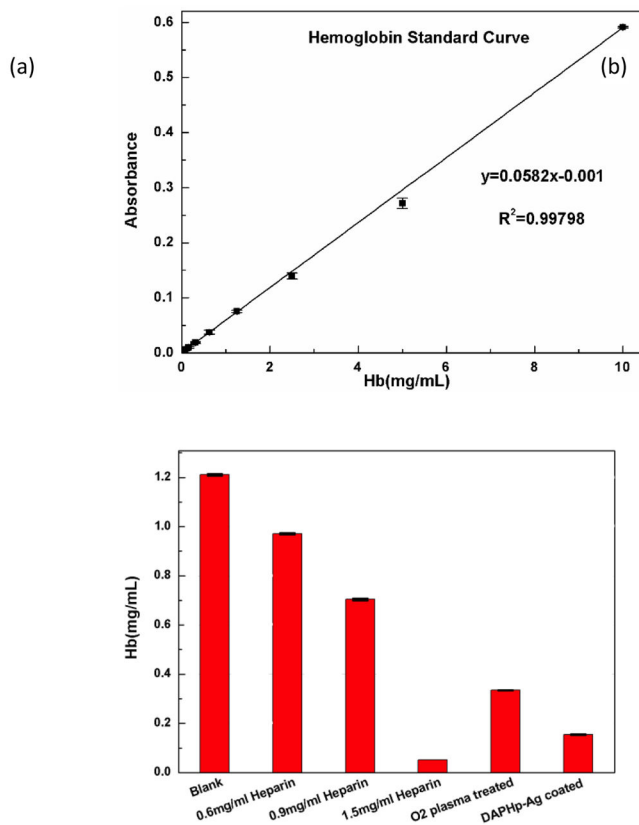


**Fig. 4.** XPS spectra of PE film (black, ■), PE film treated with O<sub>2</sub> plasma (red, ●), and DAPHP-AgNPs coated PE film (violet, ◆): (a) C1s core level spectra, (b) O1s core level spectra, (c) N1s core level spectra, (d) S2p core level spectra, (e) Ag 3d core level spectra ((a.u.) arbitrary units).

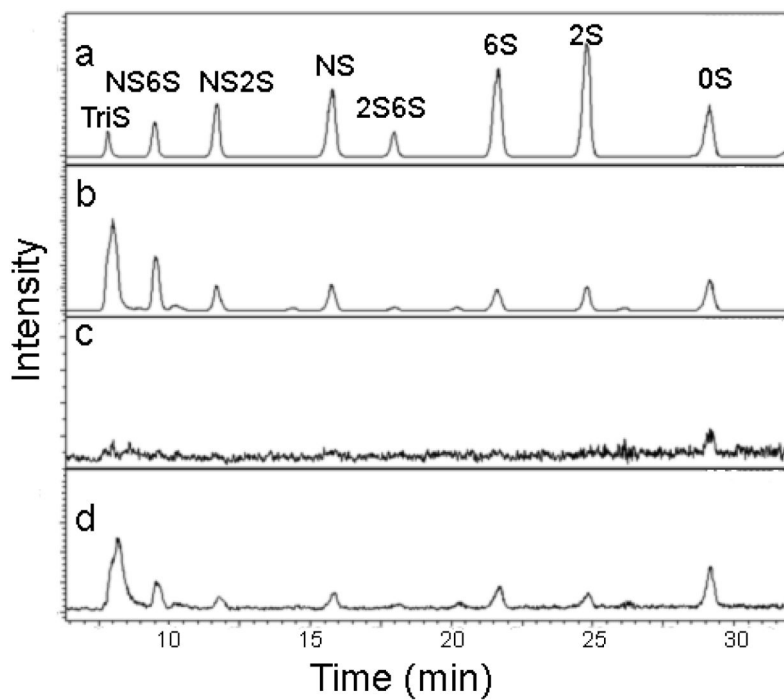




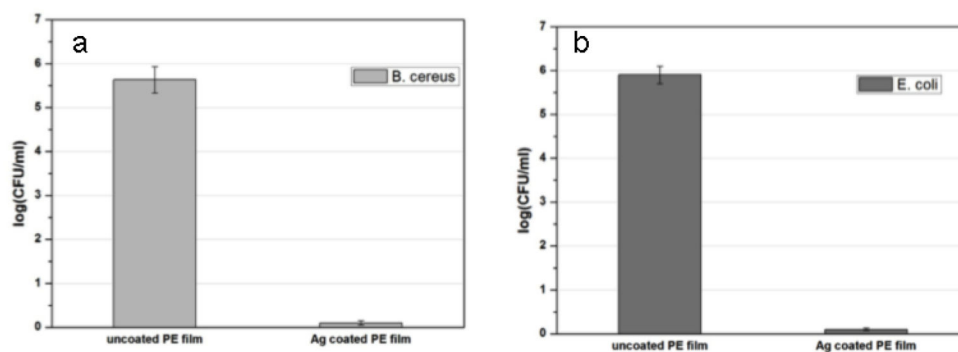
**Fig. 5.** FESEM images of DAPHP-AgNPs coated PE film (a) with O<sub>2</sub> plasma treatment (30 W, 1 min); (b) with O<sub>2</sub> plasma treatment (50 W, 1 min), the inset is the high magnification images ;(c) EDX spectra of DAPHP-AgNPs coated PE film.



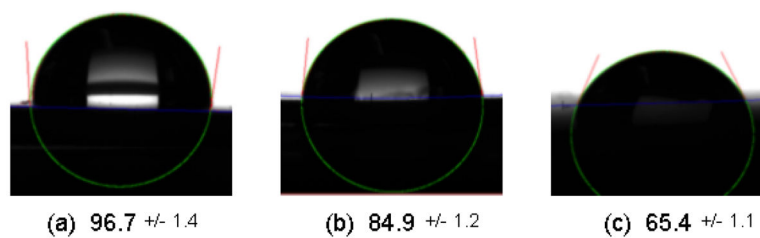
**Fig. 6.** (a) Hemoglobin (Hb) standard curve between the hemoglobin solution concentration and the absorbance. (b) Anticoagulant efficacy of the PE films.



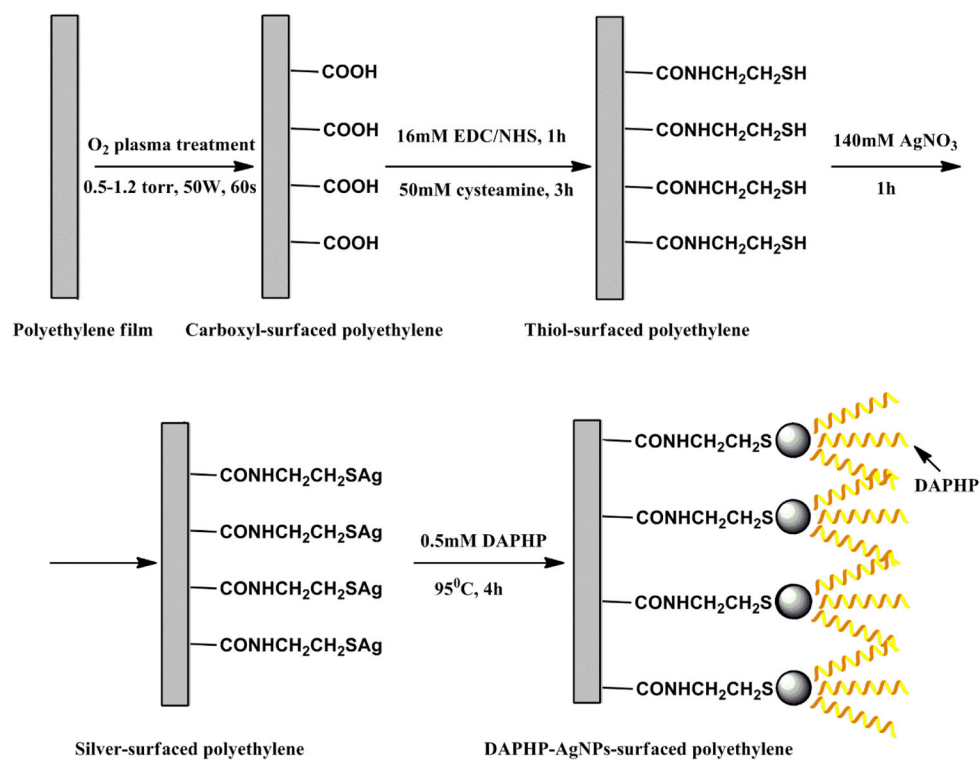
**Fig. 7.** Extracted ion chromatograph of disaccharide analysis of PE films by LC-MS. (a) disaccharide standards; (b) heparin standard; (c) PE films treated with O<sub>2</sub> plasma; (d) DAPHP-AgNPs coated PE film.



**Fig. 8.** Anti-bacterial efficacy tests on *B. cereus* (a) and *E. coli* (b) in direct contact with DAPHP-AgNPs coated and uncoated PE film. The values are the mean  $\pm$  standard deviation of three independent experiments (0.1 colonies were assumed when zero colonies were detected).



**Fig. 9.** Results of the hydrophilic experiment on (a) PE film; (b) PE film treated with O<sub>2</sub> plasma; (c) DAPHP-AgNPs coated PE film.

**Scheme 1.**

Schematic for the surface modification of PE film.

**Table 1**

The relationship between hemoglobin (Hb) solution concentration and the absorbance

Hb (mg/mL)	Absorbance			
	1	2	Average	OD-blank
10	0.627	0.629	0.628	0.591
5	0.315	0.302	0.3085	0.2715
2.5	0.173	0.181	0.177	0.14
1.25	0.111	0.114	0.1125	0.0755
0.625	0.072	0.077	0.0745	0.0375
0.312	0.055	0.057	0.056	0.019
0.156	0.046	0.048	0.047	0.01
0.0708	0.042	0.044	0.043	0.006
0	0.037	0.037	0.037	0

The anticoagulant activity of PE films treated with O<sub>2</sub> Plasma and coated with DAPHP-AgNPs

**Table 2**

Sample	Absorption			Calc. Hb (mg/mL)
	1	2	Average	
(-) Control PE film	0.104	0.109	0.1065	1.211
(+) Control heparin (0.6 mg/ml)	0.09	0.095	0.0925	0.971
(+) Control heparin (0.9 mg/ml)	0.08	0.074	0.077	0.704
(+) Control heparin (1.5 mg/ml)	0.039	0.039	0.039	---
PE Film treated with O <sub>2</sub> Plasma	0.055	0.056	0.0555	0.335
PE film coated with DAPHP-AgNPs	0.046	0.044	0.045	0.155